Organic & Biomolecular Chemistry

ROYAL SOCIETY OF CHEMISTRY

COMMUNICATION

View Article Online
View Journal | View Issue

Cite this: *Org. Biomol. Chem.*, 2024, **22**, 1993

Received 16th January 2024,
Accepted 6th February 2024

DOI: 10.1039/d4ob00191e

rsc.li/obc

Two-step access to bis-*meso*-perfluoroalkyl-corroles towards *meso*-perfluoroacyl-ABC-corroles†

Paul-Gabriel Julliard, [a] Simon Pascal, ‡[a] Olivier Siri, [a] Michel Giorgi, [b] Diego Cortés-Arriagada, [c] Luis Sanhueza*[d,e] and Gabriel Canard *[a]

A solventless and acid-catalyzed condensation of *meso*-perfluoroalkyl-dipyrromethanes with selected benzaldehydes was used to prepare ten different bilanes that were isolated before their oxidation into *trans*-A_2B-corroles bearing two *meso*-perfluoroalkyl groups. Macrocycles bearing long chains (C_3F_7 or C_7F_{15}) are key precursors to afford ABC-corroles having a *meso*-acyl substituent when subjected to a mild and basic hydrolysis affecting one of the alkyl substituents.

Corrole, the contracted homologue of the porphyrin macrocycle, is a very popular member of the porphyrinoid family and its derivatives and/or metal complexes are now used in numerous fields including, for example, sensors,[1] medicine,[2,3] catalysis[4] or the activation of small molecules.[5,6] This growing interest in the last two decades relies on the description of efficient synthetic procedures that, in a few synthetic steps, produce corroles in good yields from commercially available reagents.[7] Nevertheless, these efficient methods are mainly devoted to the preparation of corroles bearing aryl groups on their three *meso*-positions, which can be further functionalized and used to build simple to very sophisticated structures.[8,9] In contrast, the access to such macrocycles having a free *meso* position or bearing either *meso*-alkyl or *meso*-functional groups is rarely described and it usually gives low cyclization yields.[10] Because of their strong electron-withdrawing character, *meso*-perfluoroalkyl chains would be particularly attractive to increase the electro-catalytic activity of several metallocorroles whereas their lipophilicity may play a role when using such derivatives in biological studies.[11] The first example of a corrole bearing such a kind of substitution was the rhenium(v) complex of corrole **1** which was obtained through a porphyrin ring contraction (Fig. 1).[12] The access to the corresponding free base **1** was only described a decade later with a yield of 0.65%, which was increased recently and significantly up to 6% following a two-step procedure requiring the isolation of the intermediate bilane before the oxidation step.[13] Only the three other free bases **2–4** complete the rare examples of *meso*-perfluoroalkyl-corroles bearing perfluoroalkyl chains. A one-pot procedure was used to obtain 1% yield of **2** bearing three *meso*-heptafluoroalkyl chains whereas syntheses starting from *meso*-trifluoromethyl dipyrromethane (*meso*-CF_3-DPM) afforded **3** and **4** with respective yields of 5 and 3%.[14]

In the course of our research relying on the use of metallocorroles in electro-catalysis,[15] we are focusing on the preparation of *trans*-A_2B-corroles bearing two perfluoroalkyl chains on the 5,15 *meso* positions whereas the remaining one occupied by an aryl group is a potential platform for the introduction of grafting moieties and/or functional groups. Starting from *meso*-CF_3-DPM and 4-cyano-benzaldehyde, most of the previously reported synthetic procedures of *meso*-substituted

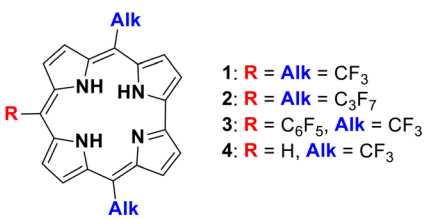

Fig. 1 Previously reported structures of *meso*-perfluoroalkylcorrole free bases.

[a]*Aix Marseille Univ., CNRS, CINAM, UMR 7325, Centre Interdisciplinaire de Nanoscience de Marseille, Campus de Luminy, 13288 Marseille cedex 09, France. E-mail: gabriel.canard@univ-amu.fr*
[b]*Aix Marseille Univ., CNRS, FSCM, Spectropole, Marseille, France*
[c]*Instituto Universitario de Investigación y Desarrollo Tecnologico, Universidad Tecnológica Metropolitana, Ignacio Valdivieso 2409, San Joaquín, Santiago, Chile*
[d]*Departamento de Ciencias Biológicas y Químicas, Facultad de Recursos Naturales, Universidad Católica de Temuco, Temuco, Chile*
[e]*Núcleo de Investigación en Bioproductos y Materiales Avanzados (BioMA), Université de Nantes, CEISAM UMR 6230, CNRS, Nantes F-44000, France*

†Electronic supplementary information (ESI) available: Experimental protocols, ^1H and ^{13}C NMR spectra, theoretical details and further DFT/TD-DFT analyses. CCDC 2267223–2267227. For ESI and crystallographic data in CIF or other electronic format see DOI: https://doi.org/10.1039/d4ob00191e

‡Present address: Laboratoire CEISAM, CNRS UMR 6230, Université de Nantes, 2, rue de la Houssinière, 44322 Nantes, France.

corroles failed to give us more than traces of the expected corrole. Inspired by the recently optimized access to corrole **1**,[13] and knowing that the bilane leading to corrole **3** was previously produced by a solventless procedure,[14b] we have investigated the solvent-free formation of bilane from *meso*-CF_3-DPM[16] and 4-cyano-benzaldehyde.

Different acids, temperatures and reaction times were used for the condensation of stoichiometric amounts of 4-cyano-benzaldehyde and *meso*-CF_3-DPM **5a** (Table S1, see the ESI†). Although the highest isolated yield of bilane **6a** (30%) was produced using 0.5 equivalents of propionic acid overnight at room temperature (RT), we chose to replace it with trifluoroacetic acid because it leads to **6a** with a similar yield (27%) in less than 5 minutes (Table S1, see the ESI†). Using these experimental conditions and starting from DPM **5a–c**[16,17] and four benzaldehyde derivatives, we obtained ten bilanes (**6a–j**) with isolated yields ranging from 11 to 40% (Table 1). Because the use of expensive PIFA as the oxidizing agent did not improve the cyclization yield of **7a** (17%), the classical oxidation procedure (DDQ, DCM, RT) was applied to these intermediates and it produced 9 to 33% yields of the ten corroles **3** and **7a–i** for which the *meso*-perfluoroalkyl moieties have one, three or seven carbon atoms (Table 1).

It was previously described that hydrolysis of the *meso*-CF_3 substituents of corrole **1** afforded the corresponding corrole bearing three *meso*-CO_2H groups. No reaction occurred when mild experimental conditions (THF, aq. NaOH, 20 mM, RT, 12 h) were used to perform the hydrolysis of the *meso*-CF_3 of **7a**, whereas the ABC corroles **8a** and **8b** bearing a *meso*-keto group were produced starting from **7d** and **7g** bearing longer alkyl chains (Scheme 1). The modest 32–35% yields result from the slow reactivity of **7d** and **7g** which are still present in the mixture after 12 hours. The stronger conditions (THF, sat. aq. NaOH, reflux, 12 h) applied to **7a** led to corrole **9** not only

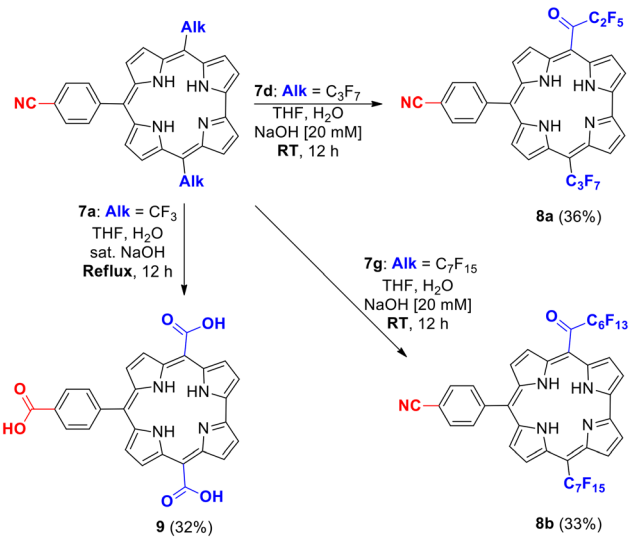

Scheme 1 Hydrolysis of the perfluoroalkyl chains of corroles **7a**, **7d** and **7g** leading to AB_2 corrole **9** and ABC corroles **8a** and **8b**.

bearing the two expected *meso*-CO_2H substituents but also an extra carboxylic group resulting from the hydrolysis of the cyano group of the aryl moiety (Scheme 1). A higher yield of corrole **9** (60%) was also obtained when trying to obtain *meso*-bis-keto corroles by applying strong experimental hydrolyzing conditions to corrole **7d**.

The impact of the *meso*-perfluoro alkyl and *meso*-perfluoro acyl chains on the physico-chemical properties of corroles **3**, **7a–i**, **8a**, **8b** and **9** was first studied by single crystal X-ray diffraction and electronic absorption and emission spectroscopy

Table 1 Synthesis of bilanes **6a–j** and their oxidation into corroles **3** and **7a–i**

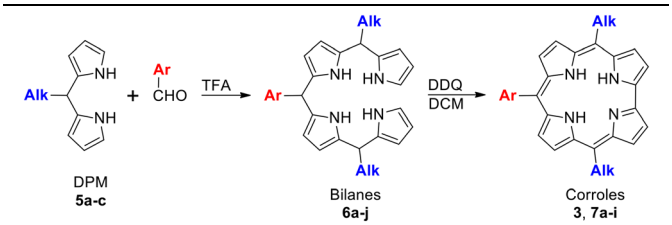

DPM	Alk	Ar	Bilanes (yields)	Corroles (yields)
5a	CF_3	*p*-CN-C_6H_4	**6a** (26%)	**7a** (18%)
	CF_3	*p*-CH_3-C_6H_4	**6b** (19%)	**7b** (13%)
	CF_3	*p*-CH_3O-C_6H_4	**6c** (40%)	**7c** (17%)
5b	C_3F_7	*p*-CN-C_6H_4	**6d** (25%)	**7d** (33%)
	C_3F_7	*p*-CH_3-C_6H_4	**6e** (17%)	**7e** (6%)
	C_3F_7	*p*-CH_3O-C_6H_4	**6f** (11%)	**7f** (24%)
5c	C_7F_{15}	*p*-CN-C_6H_4	**6g** (13%)	**7g** (7%)
	C_7F_{15}	*p*-CH_3-C_6H_4	**6h** (18%)	**7h** (11%)
	C_7F_{15}	*p*-CH_3O-C_6H_4	**6i** (15%)	**7i** (14%)
5a	CF_3	C_6F_5	**6j** (13%)	**3** (9%)

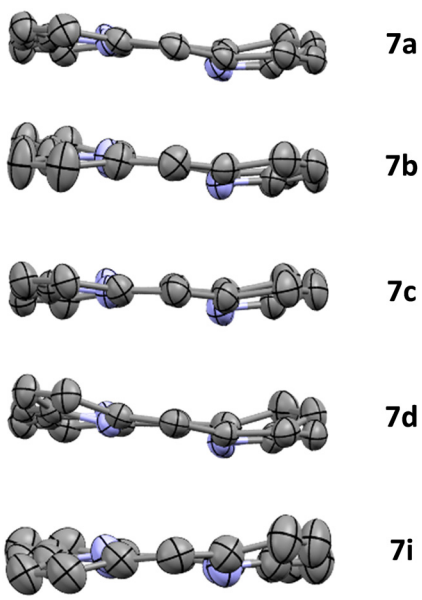

Fig. 2 Views along the C5–C15 axis of the distorted macrocycle in the single crystal X-ray diffraction structures of corroles **7a**, **7b**, **7c**, **7d** and **7i** (solvent molecules, peripheral substituents and inner hydrogen atoms are omitted for clarity).

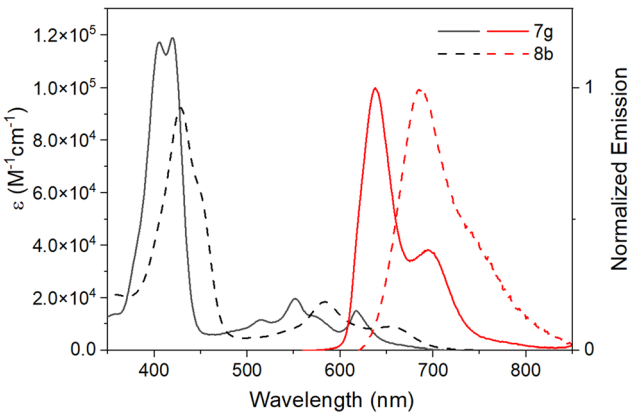

Fig. 3 Electronic absorption (black) and normalized corrected emission spectra (red) of corroles **7g** (solid lines) and **8b** (dashed lines) in aerated dichloromethane at room temperature.

supported by DFT and TD-DFT calculations. As was found for the previously reported single crystal X-ray diffraction structures of corroles **1**,[13a] **2**,[14a] **3**[14b] and **4**,[14c] the ones of corroles **7a**, **7b**, **7c**, **7d** and **7i** do not feature a particularly enhanced out of-plane distortion of the macrocycle brought by the *meso*-alkyl substituents regardless of their lengths (Fig. 2 and Fig. S1–S5 in the ESI†). As commonly observed in corrole free base structures, the deformation of the aromatic macrocycle is mainly due to the steric repulsion of the inner hydrogen atoms.

However, this distortion has a higher amplitude in the structure of **7d** in which the inner hydrogen atoms are borne by the pyrrole rings A, B and D whereas the other tautomeric form is observed in the other structures. In the five structures, hydrogen bonds involving the inner hydrogen and nitrogen atoms assemble the macrocycles into dimers that are differently packed into columns depending on the length of the alkyl chains or the presence of solvent molecules.

As for corrole **3**, the UV-visible absorption spectra of *meso*-perfluoroalkyl corroles **7a–i** feature a split Soret band in the near UV and three Q bands in the visible range (Fig. 3 and Fig. S4–S8 in the ESI†). Excitation in the Q band domain (λ = 550 nm) produces a relatively intense and structured emission in the far-red region (Table 2, Fig. 3 and Fig. S4–S8 in the ESI†) with quantum yields of *ca.* 10%. Increasing the length of the *meso*-alkyl chain produces only a trifling bathochromic shift of some of the bands displayed in the absorption and emission spectra (Table 2). In contrast, after hydrolysis, the absorption and emission spectra of the *meso*-keto corroles **8a** and **8b** are significantly red-shifted compared to those of the starting compounds **7d** and **7g** (Fig. 3 and Fig. S2–S4 in the ESI†). This bathochromic shift is also accompanied by substantial quenching of their fluorescence (Table 2).

These trends were confirmed by DFT calculations performed on corroles **7a**, **7d**, **7g**, **8a** and **8b** (see the ESI†). Increasing the lengths of the *meso*-perfluoroalkyl chain slightly stabilizes the HOMO and the LUMO energy levels of **7a**, **7d** and **7g**, which have comparable HOMO–LUMO gaps (Fig. S14 in the ESI†). These calculations reveal the role of the acyl moieties, which contribute to the distribution of the electronic density of the LUMO of **8a**, **8b**, inducing noticeably reduced HOMO–LUMO gaps compared to those of **7a**, **7d** and **7g** (Fig. S14 in the ESI†). TD-DFT methods gave convoluted UV-visible absorption spectra of the five corroles, which are in good agreement with the experimental ones and confirmed the impact of the acyl group on the red-shifted absorption spectra of **8a**, **8b** compared to those of their parent chromophores **7d** and **7g** (Fig. S16–S21 in the ESI†).

Next, cyclic voltammetry experiments conducted on all the corroles also gave evidence of the respective electron-withdrawing strength of the *meso*-alkyl and *meso*-acyl chains (Fig. S9 and S10 in the ESI†). Cyclic voltammograms of **3**, **7a–i** and **8a**, **8b** feature one irreversible reduction process and up to three

Table 2 UV-visible absorption data, fluorescence data and peak potentials (V *vs.* SCE) of corroles **3**, **7a–i**, **8a**, **8b** and **9**

	Absorption data[a]		Fluorescence data[a]		Electrochemical data[b]	
Corroles	Soret bands λ_{max} (nm) (ε (10^{-4} M^{-1} cm^{-1}))	Q bands λ_{max} (nm) (ε (10^{-4} M^{-1} cm^{-1}))	λ_{max} (nm)[c]	Φ[d]	Reduction (V)	Oxidation (V)
3	400 (14.74), 417 (13.55)	547 (1.92), 563 (1.39), 611 (1.91)	628, 681	0.09	−0.64	1.07, 1.22, 1.45
7a	402 (10.67), 420 (10.43)	513 (1.00), 549 (1.71), 614 (1.34)	639, 697	0.09	−0.55	0.96, 1.20, 1.41
7b	402 (13.25), 420 (12.12)	516 (1.16), 550 (2.16), 617 (1.58)	642, 696	0.09	−0.76	0.86, 1.04, 1.29
7c	403 (10.62), 420 (10.57)	513 (1.10), 550 (1.74), 615 (1.45)	644, 691	0.09	−0.86	0.83, 1.02, 1.24
7d	404 (12.34), 420 (12.53)	514 (1.07), 551 (1.94), 617 (1.47)	637, 695	0.12	−0.73	0.98, 1.18, 1.44
7e	404 (12.54), 419 (11.63)	515 (1.33), 552 (2.36), 620 (1.73)	641, 696	0.14	−0.59	0.90, 1.03, 1.27
7f	405 (13.50), 420 (12.10)	514 (1.14), 552 (2.07), 620 (1.50)	644, 699	0.14	−0.80	0.87, 1.02, 1.21
7g	406 (11.73), 420 (11.89)	515 (1.16), 552 (1.96), 618 (1.50)	637, 695	0.12	−0.72	0.98, 1.19, 1.36
7h	405 (11.01), 420 (10.20)	516 (1.40), 553 (2.15), 621 (1.59)	641, 695	0.13	−0.65	0.94, 1.05, 1.27
7i	407 (12.53), 420 (11.26)	516 (1.40), 553 (2.15), 621 (1.59)	644, 698	0.15	−0.59	0.91, 1.01, 1.22
8a	429 (9.37)	589 (1.81), 665 (0.93)	688	0.02	−0.34	1.02, 1.22
8b	428 (9.24)	583 (1.84), 653 (0.90)	693	0.03	−0.65	1.04, 1.20, 1.37
9	414 (4.41)[e]	574 (0.74), 639 (0.54)[e]	669[e]	0.02[e]		

[a] Recorded in air-equilibrated dichloromethane. [b] Peak potentials measured in dichloromethane containing 0.1 M [(^{n}Bu$_4$N)PF$_6$] (scan rate of 100 mV s^{-1}). [c] λ_{max} for the bands derived from corrected emission spectra. [d] Luminescence quantum yields obtained using tetraphenylporphyrin (TPP) in aerated acetonitrile as a standard (Φ = 0.15).[20] [e] Recorded in air-equilibrated methanol.

irreversible oxidation ones. It was shown that the irreversibility of these redox processes arises from the gain or loss of inner protons when oxidizing or reducing corrole free bases.[18] Comparing the peak potentials of the first reduction of each corrole is problematic because it produces very large waves under our experimental conditions (DCM, RT, scan rate of 100 mV s^{-1}).

In the anodic range, a slight shift of 20 mV affects the value of the first oxidation potential when increasing the length of the perfluoro-alkyl group from **7a** to **7d** and to **7g** (Table 2). In the same way, corroles **8a** and **8b** are harder to oxidize by *ca.* 50 mV than their parent corroles **7d** and **7g** (Table 2). The amplitude of these shifts is small but still reflects the difference between Hammett constants of analogous perfluoro alkyl and acyl groups ($\sigma_p(CF_2CF_3) = 0.52 < \sigma_p(COCF_2CF_2CF_3) = 0.79 \sim \sigma_p(COCF_3) = 0.80$).[19]

Metallocorroles are particularly efficient in the electrocatalytic reduction of small molecules, which requires the introduction of strongly electron withdrawing substituents on the macrocycle peripheral positions which decrease the associated activation potentials.[6,21] To this purpose, we describe herein a two-step access to corroles displaying two *meso*-perfluoro-alkyl groups. The formation of the bilane was conducted under acidic neat conditions without any detectable acidolysis/recombination of the polypyrrolic oligomers. After their crucial isolation, the oxidation of these precursors led to the formation of ten corroles substituted with two *meso*-alkyl groups having one, three or seven carbon atoms. If longer alkyl chains do not tune significantly the physico-chemical properties of the macrocycles, they are of particular interest because their hydrolysis has led to unprecedented ABC-corroles bearing *meso*-perfluoro acyl groups. Two examples of such derivatives were prepared and characterized, highlighting the electron-accepting strength of such *meso*-acyl moieties, which are also responsible for red-shifted light absorption and emission properties.

Conflicts of interest

There are no conflicts to declare.

Acknowledgements

This contribution comes within the framework of the ECOS Sud-Chile project no. C19E07 supported by the Chilean Agencia Nacional de Investigación y Desarrollo (ANID), the French Ministère de l'Enseignement Supérieur, de la Recherche et de l'Innovation (MESRI) and the French Ministère de l'Europe et des Affaires Étrangères (MEAE). This work was supported in France by the Centre National de la Recherche Scientifique (CNRS) and by the MESRI. PGJ acknowledges the MESRI (PhD grant). LS and DCA are thankful for the computational resources through the CONICYT-FONDEQUIP-EQM180180 and acknowledge ANID/FONDECYT projects 11181187 and 1210355, respectively.

Notes and references

1 C. Di Natale, C. P. Gros and R. Paolesse, *Chem. Soc. Rev.*, 2022, **51**, 1277–1335.
2 R. D. Teo, J. Y. Hwang, J. Termini, Z. Gross and H. B. Gray, *Chem. Rev.*, 2017, **117**, 2711–2729.
3 S. M. M. Lopes, M. Pineiro and T. M. V. D. Pinho e Melo, *Molecules*, 2020, **25**, 3450.
4 I. Aviv and Z. Gross, *Chem. Commun.*, 2007, 1987–1999.
5 V. A. Vaillard, P. D. Nieres, S. E. Vaillard, F. Doctorovich, B. Sarkar and N. I. Neuman, *Eur. J. Inorg. Chem.*, 2022, e202100767.
6 Y. Li, N. Wang, H. Lei, X. Li, H. Zheng, H. Wang, W. Zhang and R. Cao, *Coord. Chem. Rev.*, 2021, **442**, 213996.
7 R. Orłowski, D. Gryko and D. T. Gryko, *Chem. Rev.*, 2017, **117**, 3102–3137.
8 J. P. Collman and R. A. Decréau, *Org. Lett.*, 2005, **7**, 975–978.
9 L. Flamigni and D. T. Gryko, *Chem. Soc. Rev.*, 2009, **38**, 1635–1646.
10 (*a*) J. Sankar, V. G. Anand, S. Venkatraman, H. Rath and T. K. Chandrashekar, *Org. Lett.*, 2002, **4**, 4233–4235; (*b*) G. Canard, D. Gao, A. D'Aléo, M. Giorgi, F.-X. Dang and T. S. Balaban, *Chem. – Eur. J.*, 2015, **21**, 7760–7771; (*c*) S. Ooi, T. Yoneda, T. Tanaka and A. Osuka, *Chem. – Eur. J.*, 2015, **21**, 7772–7779; (*d*) A. Kumar, P. Yadav, M. Majdoub, I. Saltsman, N. Fridman, S. Kumar, A. Kumar, A. Mahammed and Z. Gross, *Angew. Chem., Int. Ed.*, 2021, **60**, 25097–25103.
11 (*a*) K. Sudhakar and P. K. Panda, *ACS Appl. Energy Mater.*, 2022, **5**, 13492–13500; (*b*) H. C. Honig, A. Friedman, N. Zion and L. Elbaz, *Chem. Commun.*, 2020, **56**, 8627–8630; (*c*) B. E. Smart, *J. Fluorine Chem.*, 2001, **109**, 3–11.
12 M. K. Tse, Z. Zhang and K. S. Chan, *Chem. Commun.*, 1998, 1199–1200.
13 (*a*) C. K. E. Thomas, J. Conradie, L. K. Hansen and A. Ghosh, *Inorg. Chem.*, 2011, **50**, 3247–3251; (*b*) Q.-C. Chen, M. Soll, A. Mizrahi, I. Saltsman, N. Fridman, M. Saphier and Z. Gross, *Angew. Chem., Int. Ed.*, 2018, **57**, 1006–1010; (*c*) P. Yadav, S. Khoury, A. Mahammed, M. Morales, S. C. Virgil, H. B. Gray and Z. Gross, *Org. Lett.*, 2020, **22**, 3119–3122.
14 (*a*) L. Simkhovich, I. Goldberg and Z. Gross, *J. Inorg. Biochem.*, 2000, **80**, 235–238; (*b*) R. Goldschmidt, I. Goldberg, Y. Balazs and Z. Gross, *J. Porphyrins Phthalocyanines*, 2006, **10**, 76–86; (*c*) P. Yadav, S. Khoury, N. Fridman, V. K. Sharma, A. Kumar, M. Majdoub, A. Kumar, Y. Diskin-Posner, A. Mahammed and Z. Gross, *Angew. Chem., Int. Ed.*, 2021, **60**, 12829–12834.
15 P.-G. Julliard, M. Hanana, L. Alvarez, R. Cornut, B. Jousselme, G. Canard and S. Campidelli, *Energy Fuels*, 2023, **37**, 684–692.
16 (*a*) W. Dmowski, K. Piasecka-Maciejewska and Z. Urbanczyk-Lipkowska, *Synthesis*, 2003, 841–844; (*b*) W. Dmowski, K. Piasecka-Maciejewska and Z. Urbańczyk-Lipkowska, *Kem. Ind.*, 2004, **53**, 339–341.

17 P.-G. Julliard, S. Pascal, O. Siri, D. Cortés-Arriagada, L. Sanhueza and G. Canard, *C. R. Chim.*, 2021, **24**, 27–45.
18 J. Shen, J. Shao, Z. Ou, E. Wembo, B. Koszarna, D. T. Gryko and K. M. Kadish, *Inorg. Chem.*, 2006, **45**, 2251–2265.
19 C. Hansch, A. Leo and R. W. Taft, *Chem. Rev.*, 1991, **91**, 165–195.
20 A. M. Brouwer, *Pure Appl. Chem.*, 2011, **83**, 2213–2228.
21 H. Lei, X. Li, J. Meng, H. Zheng, W. Zhang and R. Cao, *ACS Catal.*, 2019, **9**, 4320–4344.